"Discontinuous Galerkin method for 1D river flows"

Draoui, Insaf ; Lambrechts, Jonathan ; Legat, Vincent ; Soares Frazao, Sandra ; Hoitink, Ton (A.J.F.) ; Deleersnijder, Eric

ABSTRACT

We study the stability of various formulations of the momentum conservation equation for 1D flows in real rivers. The 1D Saint-Venant equations are solved using a Discontinuous Galerkin numerical method and applied to relevant test cases. We explain how to deal with arbitrary cross sections. The water level and water depth as direct terms in the equations hamper the appropriate treatment of arbitrary cross sectional areas. Applying Newton s second law of motion to a control volume leads to a more stable formulation. The modelling of connections of several channels is also addressed with a formulation based on curvilinear coordinates. The 1D model in this case is validated based on a comparison with a 2D model for the different configurations.

CITE THIS VERSION

River Flow 2020 – Uijttewaal et al (eds)
© 2020 Taylor & Francis Group, London, ISBN 978-0-367-62773-7

Discontinuous Galerkin method for 1D river flows

Insaf Draoui, Jonathan Lambrechts, Vicent Legat & Sandra Soares-Frazao
Université catholique de Louvain, Institute of Mechanics, Materials and Civil Engineering (IMMC), Louvain-la-Neuve, Belgium

Ton Hoitink
Department of Environmental Sciences, Hydrology and Quantitative Water Management, Wageningen University & Research, Wageningen, The Netherlands

Eric Deleersnijder
Université catholique de Louvain, Institute of Mechanics, Materials and Civil Engineering (IMMC) & Earth and Life Institute (ELI), Louvain-la-Neuve, Belgium

ABSTRACT: We study the stability of various formulations of the momentum conservation equation for 1D flows in real rivers. The 1D Saint-Venant equations are solved using a Discontinuous Galerkin numerical method and applied to relevant test cases. We explain how to deal with arbitrary cross sections. The water level and water depth as direct terms in the equations hamper the appropriate treatment of arbitrary cross sectional areas. Applying Newton s second law of motion to a control volume leads to a more stable formulation. The modelling of connections of several channels is also addressed with a formulation based on curvilinear coordinates. The 1D model in this case is validated based on a comparison with a 2D model for the different configurations.

1 INTRODUCTION

Rivers generally exhibit a simple dynamics, which can often be dealt with satisfactorily by having recourse to 1D models. Numerical resolution of the governing equations can be achieved using several methods such as finite-difference (Cunge and Wegner 1964), finite-element (FE) (Szymkiewicz 1991, Katsaounis and Makridakis 2003) and finite-volume (FV) methods. The latter are known for their ability to reproduce discontinuous solutions (Sanders 2001, Franzini and Soares-Frazão 2016). The discontinuous Galerkin finite element (DG) method can be seen as a combination of the finite element and the finite volume methods. It allows more flexibility, merging the discontinuous -or piecewise continuous- approximation of solution (FE) and solving the edges fluxes ensuring an optimal stability (FV).

Here the DG method is evaluated for modelling 1D flows in rivers. Most of the previous validation test cases were made in channels with prismatic or non prismatic rectangular or trapezoidal cross sections. In such cases the definition of variables is straightforward (the relation between cross section, the channel width and water depth is known). Some DG studies focused on rivers (Lai and Khan 2012, Pham Van et al. 2016). In such configurations the geometry of the cross section is arbitrary and presents high variations. As a result the intermediate variables of the momentum equation (water depth, water level, bed level) should be carefully defined.

For its natural ability to conserve mass, the conservative form of the equations is adopted. The flux term can be written in several forms. It is seen, however, that not all of them lead to stable and accurate numerical results. This study analyses several formulations, trying to

present more details about the numerical treatment of the data in the case of an arbitrary geometry.

2 BASIC EQUATIONS

For elongated, shallow domains, it is customary to simplify the full 3D Navier-Stokes equations to a system of 1D, cross section-integrated equations, yielding:

$$\frac{\partial \mathbf{U}}{\partial t} + \frac{\partial \mathbf{F}(\mathbf{U})}{\partial x} = \mathbf{S}(\mathbf{U}) \tag{1}$$

where t and x denote the time and the along-flow coordinate; $\mathbf{U} = (A(x,t), Q(x,t))^t$ is the vector of unknowns with A the cross-sectional area and Q the volumetric flow rate, whilst $\mathbf{F}(\mathbf{U})$ and $\mathbf{S}(\mathbf{U})$ are the relevant fluxes and source terms. Several choices of variables and parameters lead to mathematically equivalent partial differential equations. However, in the discrete form the choice of variables and parameters making up the flux and source terms has a crucial impact on stability. Several formulations of flux and source terms will be presented and analysed in what follows.

A seemingly simple formulation reads:

$$\begin{bmatrix} \frac{\partial A}{\partial t} \\ \frac{\partial Q}{\partial t} \end{bmatrix} + \begin{bmatrix} \frac{\partial Q}{\partial x} \\ \frac{\partial}{\partial x}\left(\frac{Q^2}{A}\right) \end{bmatrix} = \begin{bmatrix} 0 \\ gA\frac{\partial \eta}{\partial x} - gS \end{bmatrix} \tag{2}$$

where $H(x,t)$, $\eta(x,t)$ and $h(x)$ are respectively the total water depth, the mean water level and bed level as represented in Figure 1. S is the slope of the energy line (i.e. the friction induced head loss per unit distance). The Manning formulation for $S(A,Q)$ is:

$$S = n^2 \frac{|Q|Q}{A(H^*)^{4/3}}$$

with $H^* = \frac{A}{b^*}$ the effective depth, and $b^*(x,t) \widehat{=} b(x, z = \eta(x,t))$ the free surface width.

In the discrete form the stabilization affects only the flux term. Hence, the water level gradient that is an important physical driving force is not impacted. A special treatment should be given to the flux and source terms (Lai and Khan 2012, Pham Van et al. 2016).

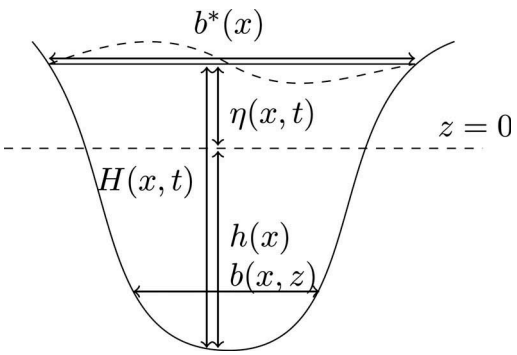

Figure 1. The 1D notations in a river cross section: $\eta(x,t)$ is the mean free surface level and $h(x)$ is the bed level measured to the deepest cross section point. The water depth $H(x,t)$ is defined as $H(x,t) \widehat{=} \eta(x,t) + h(x)$. $b^*(x)$ is the free surface width and $b(x,z)$ is the cross section width at altitude z.

An alternative would be to include directly the water level gradient in the flux term for the momentum conservation equation, yielding:

$$\frac{\partial Q}{\partial t} + \frac{\partial}{\partial x}\left(\frac{Q^2}{A} + gA\eta\right) = g\eta\frac{\partial A}{\partial x} - gS \tag{3}$$

Once discretized, this formulation may lead to some stability issues. The water level η being defined to an arbitrary level, in a discrete form passing from a level to another introduces an extra constant in the flux term. The choice of an optimal reference level is far from straightforward.

The water depth, being independent from the reference level, offers an attractive alternative. Since by definition the water depth is $H \widehat{=} \eta + h$ (Figure 1), the obtained momentum conservation equation is:

$$\frac{\partial Q}{\partial t} + \frac{\partial}{\partial x}\left(\frac{Q^2}{A} + gAH\right) = gH\frac{\partial A}{\partial x} + gA\frac{dh}{dx} - gS \tag{4}$$

Since in a real river the bed level is related to the deepest point, its evolution along the river presents high variations especially near meanders. If the flux term is stable, the source term is problematic in this configuration as both H and h are highly varying in realistic rivers.

An alternative way to derive the momentum conservation equation consists in applying Newton's 2^{nd} law to a control volume. Then, we obtain:

$$\frac{\partial Q}{\partial t} + \frac{\partial}{\partial x}\left(\frac{Q^2}{A} + \frac{P}{\rho}\right) = gA\frac{dh}{dx} - gS + \frac{F_{lat}}{\rho} \tag{5}$$

where $P = \rho g \int_0^H (H - z) b \, dz$ refers to the frontal hydrostatic pressure force applied to the upstream and downstream cross sections, while $F_{lat} = \rho g \int_0^H (H - z) \frac{\partial b}{\partial x} dz$ is the projection along the x axis of the wall pressure force induced by width variation per unit length.

The pressure and wall pressure being integral variables, they are less sensitive to the reference level. The zero of the integral is associated to the bottom of the cross section (Petaccia et al. 2013). Considering a global reference level (associated to z' in Figure 2) the pressure force is seen to be invariant:

$$\int_0^{H'} (H' - z') b(x, z') dz' = \underbrace{\int_0^h (H' - z') 0 dz'}_{0} + \underbrace{\int_h^{H'} (H' - z') b(x, z') dz'}_{= \int_0^H (H - z) b(x,\, z) dz}$$

Formulation (5) is adopted and validated hereinafter.

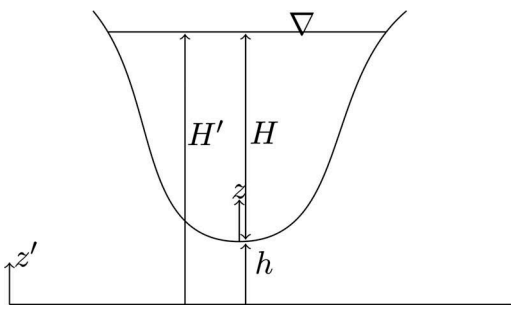

Figure 2. Notation and datum for the pressure force calculation in an arbitrary geometry.

3 NUMERICAL METHOD

The computational domain Ω is divided into a set of N_e non overlapping elements Ω_e. On the basis of equation (1), we seek an approximation U_h of U in the finite dimensional space of polynomials on element Ω_e of degree at most 1. With ϕ_i the set of independent shape functions and U_i^e the new unknown nodal values, the approximate solution reads:

$$U|_{\Omega_e} \simeq U_h|_{\Omega_e} = \sum_{i=1}^{2} \phi_i \mathbf{U}_i^e \tag{6}$$

3.1 *Numerical flux*

The weak formulation is obtained by multiplying equation (1) by test functions $\hat{\mathbf{u}} \in \mathcal{U}_1^h$. In the standard DG method the test functions are the local basis functions ϕ_i. Integrating over Ω_e we obtain:

$$< \frac{\partial \mathbf{U}_h}{\partial t} \hat{\mathbf{u}} >_{\Omega_e} + \tilde{\mathbf{F}}_2 - \tilde{\mathbf{F}}_1 - < \mathbf{F}(\mathbf{U}_h) \frac{\partial \hat{\mathbf{u}}}{\partial x} >_{\Omega_e} = < \mathbf{S}(\mathbf{U}_h) \hat{\mathbf{u}} >_{\Omega_e} \tag{7}$$

The approximate solution $\mathbf{U}_h$ is discontinuous at the element edges as represented in Figure 3. The integral $< \frac{\partial}{\partial x} (\mathbf{F}(\mathbf{U}_h) \hat{\mathbf{u}}) >_{\Omega_e}$ yields $\tilde{\mathbf{F}}_2 - \tilde{\mathbf{F}}_1$, which takes into account both the left and right values of the node. At each node we create a Riemann problem. The system ((2)) can be transformed into a linearised set of two independent transport equations. The non-conservative equations is rewritten in the basis formed by the eigenvectors of the Jacobian matrix of the flux $\mathbf{J} = \frac{\partial F(U)}{\partial U}$ to obtain the following characteristic form:

$$\begin{bmatrix} \frac{\partial W1}{\partial t} \\ \frac{\partial W2}{\partial t} \end{bmatrix} + \begin{bmatrix} \frac{Q_0}{A_0} - \sqrt{\frac{gA_0}{b^*}} & 0 \\ 0 & \frac{Q_0}{A_0} + \sqrt{\frac{gA_0}{b^*}} \end{bmatrix} \begin{bmatrix} \frac{\partial W1}{\partial x} \\ \frac{\partial W2}{\partial x} \end{bmatrix} = \begin{bmatrix} -gA \frac{dh}{dx} + gS \\ gA \frac{dh}{dx} - gS \end{bmatrix} \tag{8}$$

$$W1 = (\frac{Q_0}{A_0} + \sqrt{\frac{gA_0}{b^*}})A - Q \quad \text{and} \quad W2 = (-\frac{Q_0}{A_0} + \sqrt{\frac{gA_0}{b^*}})A + Q$$

where A_0 and Q_0 are the mean values between the left $U_{\mathbf{2}}^e$ and right $U_{\mathbf{1}}^{e+\mathbf{1}}$ nodal values. The Riemann variables W_1 and W_2 being invariant, the Riemann unknown U^* on elements Ω_e and Ω_{e+A} is to be determined, its unicity is the result of the volume flux conservation $Q_e^* = Q_{e+1}^*$ and the conservation of energy that simplifies to the conservation of the water depth in subcritical flows $A_e^* = A_{e+1}^*$.

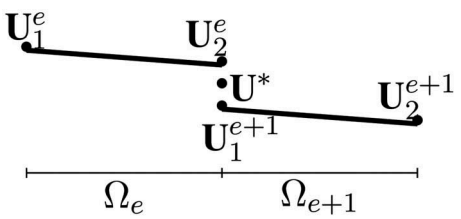

Figure 3. Discontinuous approximation U_h on consecutive elements Ω_e and Ω_{e+1}.

The obtained system reads:

$$\text{On } \Omega_e\text{: } -A^*\left(\frac{Q_0}{A_0}+\sqrt{\frac{gA_0}{b^*}}\right)+Q^*=-A_2^e\left(\frac{Q_0}{A_0}+\sqrt{\frac{gA_0}{b^*}}\right)+Q_2^e$$

$$\text{On } \Omega_{e+1}\text{: } A^*\left(-\frac{Q_0}{A_0}+\sqrt{\frac{gA_0}{b^*}}\right)+Q^*=A_1^{e+1}\left(-\frac{Q_0}{A_0}+\sqrt{\frac{gA_0}{b^*}}\right)+Q_1^{e+1}$$

The characteristic variable U^* is then used for evaluating the numerical flux $\mathcal{F}=F(U^*)\hat{n}$.

3.2 *Junction treatment*

The fluid flow at a branching point presents a 3D dynamics. Secondary circulations are observed. The 1D model is clearly not able to capture the details of this 3D dynamics. Nevertheless if only the flow rate share in the different branches and the water level far from the connection point are of interest, a simplified 1D model may be sufficient to obtain acceptable results. At the connection point six characteristic variables are to be determined, based on the same reasoning as that used for evaluating fluxes. The volume flux conservation reads here:

$$Q_i^*=Q_k^*+Q_j^* \tag{9}$$

The velocity is subject to variations in the different branches. The energy conservation reads in its full formulation:

$$h_i+\frac{A_i^*}{b_i^*}+\frac{Q_i^2}{2gA_i^2}=h_j+\frac{A_j^*}{b_j^*}+\frac{Q_j^2}{2gA_j^2}=h_k+\frac{A_k^*}{b_k^*}+\frac{Q_k^2}{2gA_k^2} \tag{10}$$

In the case of a subcritical bifurcation as represented in Figure 4, with no bathymetry jump at the connection point, the system of equations reads:

$$\begin{cases} Q_i^*=Q_i+\left(\frac{Q_0}{A_0}-\sqrt{\frac{gA_0}{b_i^*}}\right)(A_i^*-A_2^i) \\ Q_j^*=Q_j+\left(\frac{Q_0}{A_0}+\sqrt{\frac{gA_0}{b_j^*}}\right)(A_j^*-A_j) \\ Q_k^*=Q_k+\left(\frac{Q_0}{A_0}+\sqrt{\frac{gA_0}{b_k^*}}\right)(A_k^*-A_k) \\ Q_i^*=Q_j^*+Q_k^* \\ \frac{Q_i^2}{2gA_i^2}+\frac{A_i^*}{b_i^*}=\frac{Q_j^2}{2gA_j^2}+\frac{A_j^*}{b_j^*} \\ \frac{Q_i^2}{2gA_i^2}+\frac{A_i^*}{b_i^*}=\frac{Q_k^2}{2gA_k^2}+\frac{A_k^*}{b_k^*} \end{cases} \tag{11}$$

where Q_0 and A_0 are still the arithmetic average of the water volumetric flow rate and cross-sectional area.

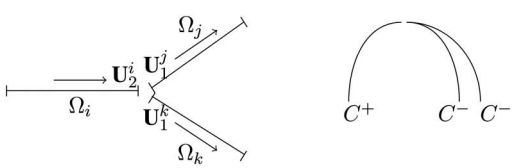

Figure 4. Characteristics at the subcritical bifurcation: in the main branch Ω_i the information is provided by the forward travelling wave on C^+ characteristic, the needed values at cells Ω_j and Ω_k are carried by the backward wave over C^- characteristic.

4 NUMERICAL RESULTS

We now examine the performance of the abovementioned numerical scheme for variable geometry and topography. The governing equations are solved by means of an explicit DG-FEM.

The water at rest test aims to evaluate the well-balance property of our numerical scheme. We consider a rectangular $1500m$ frictionless channel length. The width and bed level values at distinct points along the channel can be found in Delis (2003). Applying simple non-reflecting boundary conditions (zero entering discharge and the initial water depth downstream) the zero discharge is conserved to a 10^{-11} precision.

As suggested in Macdonald (1996) we tackle two test cases corresponding to non prismatic channels with rectangular and trapezoidal cross sections. For a steady state, based on the geometry the bed slope leading to a specific water level can be analytically determined. Details concerning the bottom width (B_0), channel length (L) manning coefficient (n), bed slope expression $\frac{dh}{dx}$ and boundary conditions can be found in the same reference. The root mean square deviation from the analytical solution is evaluated to validate the convergence of the scheme for various mesh sizes: $(0.5m, 1m, 2m, 4m, 8m, 16m, 32m)$.

Rectangular non prismatic cross section: the channel is $200m$ long with a rectangular cross section. The water depth is:

$$H(x) = 0.9 + 0.3\,exp\left(-20\left(\frac{x}{200} - \frac{1}{2}\right)^2\right)$$

The RMS error and the cross sectional area results are represented in Figure 5.

Trapezoidal non prismatic cross section: the channel is $400m$ long with a trapeze side slope of $1/2$. The water depth is:

$$H(x) = 0.9 + 0.3\,exp\left(-40\left(\frac{x}{400} - \frac{1}{3}\right)^2\right) + 0.2\,exp\left(-35\left(\frac{x}{400} - \frac{2}{3}\right)^2\right)$$

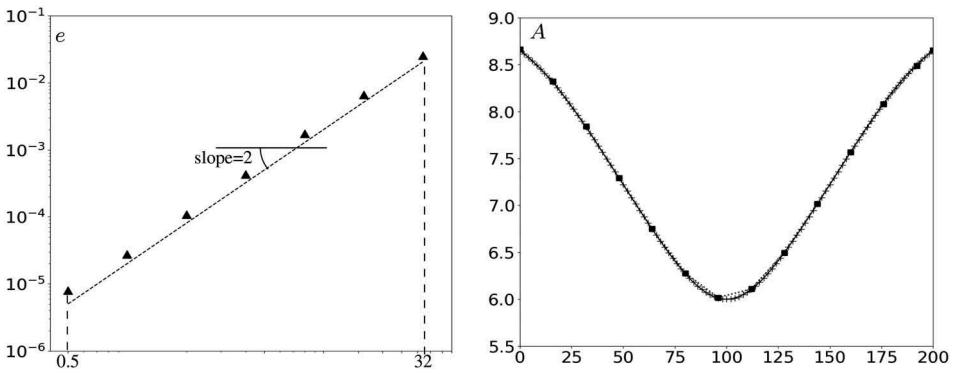

Figure 5. The RMS error (e) for steady flow in rectangular non-prismatic channel as function of mesh size (dx). On the right side the cross sectional area A along the channel results for a $dx = 2$ (+), $dx = 16$ (.....) and analytical solution (−).

In the case of a channel junction additional issues are related to bifurcations rather than confluences. In a bifurcation the flow rate division is influenced by many parameters such as the bed slope, bed roughness, channel width while in a confluence the incoming water flux is simply cumulated to continue its way in the main branch. For this reason the test cases presented below will focus on discharge division in a bifurcation.

Table 1. Key parameters for the numerical test cases related to a bifurcation: channel width $B_0(m)$, bed slope $S_0 = \frac{dh}{dx}(^{o}/_{oo})$, Manning coefficient n. The flow rate division in the sub-channels obtained with the 1D and 2D models is presented .

channel P		channel S1					channel S2				
S_0	n	B_0	S_0	n	1D	2D	B_0	S_0	n	1D	2D
0.5	0.03	50	0.5	0.02	51.90	51.33	50	0.5	0.03	36.09	36.67
5	0.03	50	2	0.03	49.67	48.43	50	5	0.03	38.33	39.57
5	0.03	50	5	0.03	22.21	23.67	60	5	0.03	65.79	64.33
0.18 ($AS_0 = S$)	0.03	50	0.18	0.03	44	-	50	0.18 ($AS_0 = S$)	0.03	44	-

Accordingly several tests were run in which one of the parameters is modified at a time. In the absence of an analytical solution validation will be done based on a comparison with 2D model results for identical configurations.

The domain consists of three branches P, S_1 and S_2, whose length is $1500m$. The main branch P is $100m$ wide. The same boundary conditions were applied for all the tests, i.e. an incoming flow rate of $88m^3s^{-1}$ and a water depth of $1.5m$ downstream. Tests details and results are summarized in Table 1.

The 4^{th} test admits an analytical solution. Since the source term is zero, the water depth is conserved in all channels.

5 DISCUSSION AND CONCLUSION

This study underscores the importance of two basic points. First when solving a river flow problem in a discrete domain the simplest formulation may create several problems as discussed in Section 2. For the 1D Saint-Venant equations even though the pressure integrals may look expensive in terms of CPU time they are offering more stable flux and source terms. In addition the pressure force can be calculated in advance (as a function of the non varying geometry) per depth level to be used with different flow conditions, allowing for an optimization of the computing time. Secondly when modelling a river connection, the results obtained should be analysed with caution.

Both the 1D and 2D models have limits. For the 1D model, the first issue is related to the fact that the coordinate x is the curvilinear abscissa along the river, implying that the model is not able to capture the angle between the connection branches that can be easily seen in the (x,y) plan used in the 2D model. A comparison between 1D and 2D results for the different tests shows that in addition to the parameters variations the direction of the branches may have a significant influence, too. In a subcritical flow the difference can be acceptable but when the Froude number approaches unity the orientation has a significant impact on the water flow rate division. The 2D model also has proven its limits as for the representation of the cross section geometry which is why the validation was done in rectangular channels.

REFERENCES

J. A. Cunge and M. Wegner. Intégration numérique des équations d'écoulement de Barré de Saint-Venant par un schéma implicite de différences finies. *La Houille Blanche*, 0 (1): 033–39, 1964.

A. Delis. Improved application of the hlle riemann solver for the shallow water equations with source terms. *Communications in Numerical Methods in Engineering*, 190 (1): 0 59–83, 2003.

F. Franzini and S. Soares-Frazão. Efficiency and accuracy of Lateralized HLL, HLLS and augmented Roe's scheme with energy balance for river flows in irregular channels. *Applied Mathematical Modelling*, 400 (17-18): 07427–7446, 2016.

T. Katsaounis and C. Makridakis. Relaxation models and finite element schemes for the shallow water equations. In *Hyperbolic Problems: Theory, Numerics, Applications*, 621–631. Springer, 2003.

W. Lai and A. Khan. Discontinuous galerkin method for 1d shallow water flows in natural rivers. *Engineering Applications of Computational Fluid Mechanics*, 60 (1):0 74–86, 2012.

I. MacDonald. *Analysis and computation of steady open channel flow*. PhD thesis, Citeseer, 1996.

G. Petaccia, L. Natale, F. Savi, M. Velickovic, Y. Zech, and S. Soares-Frazão. Flood wave propagation in steep mountain rivers. *Journal of Hydroinformatics*, 150 (1): 0120–137, 2013.

C. Pham Van, B. de Brye, E. Deleersnijder, A. Hoitink, M. Sassi, B. Spinewine, H. Hidayat, and S. Soares-Frazão. Simulations of the flow in the Mahakam river–lake–delta system, Indonesia. *Environmental Fluid Mechanics*, 160 (3): 0603–633, 2016.

B. F. Sanders. High-resolution and non-oscillatory solution of the st. venant equations in non-rectangular and non-prismatic channels. *Journal of Hydraulic Research*, 390 (3): 0321–330, 2001.

R. Szymkiewicz. Finite-element method for the solution of the Saint-Venant equations in an open channel network. *Journal of Hydrology*, 1220 (1-4): 0275–287, 1991.